Article

Self-Assembly of Lyotropic Chromonic Liquid Crystal Sunset Yellow and Effects of Ionic Additives

Heung-Shik Park, Shin-Woong Kang, Luana Tortora, Yuriy Nastishin,
Daniele Finotello, Satyendra Kumar, and Oleg D. Lavrentovich

More About This Article

Additional resources and features associated with this article are available within the HTML version:

- Supporting Information
- Access to high resolution figures
- Links to articles and content related to this article
- Copyright permission to reproduce figures and/or text from this article

View the Full Text HTML

Self-Assembly of Lyotropic Chromonic Liquid Crystal Sunset Yellow and Effects of Ionic Additives

Heung-Shik Park,[†] Shin-Woong Kang,[‡] Luana Tortora,[†] Yuriy Nastishin,[†,§] Daniele Finotello,[‡] Satyendra Kumar,[†,‡,||] and Oleg D. Lavrentovich*,[†,‡]

Liquid Crystal Institute and Chemical Physics Interdisciplinary Program and Department of Physics, Kent State University, Kent, Ohio 44242, Institute of Physical Optics, 23 Dragomanov Street, Lviv 79005, Ukraine, and Division of Materials Research, National Science Foundation, Arlington, Virginia 22230

Received: May 29, 2008; Revised Manuscript Received: October 1, 2008

Lyotropic chromonic liquid crystals (LCLCs) are formed by molecules with ionic groups at the periphery that associate into stacks through noncovalent self-assembly while in water. The very existence of the nematic (N) phase in the typical LCLC, the dye Sunset Yellow (SSY) is a puzzle, as the correlation length associated with the stacking, as measured in the X-ray experiments, is too short to explain the orientational order by the Onsager model. We propose that the aggregates can be more complex than simple rods and contain "stacking faults" such as junctions with a shift of neighboring molecules, 3-fold junctions, etc. We study how ionic additives, such as salts of different valency and pH-altering agents, alter the N phase of SSY purified by recrystallization. The additives induce two general trends: (a) stabilization of the N phase, caused by the mono and divalent salts (such as NaCl), and evidenced by the increase of the N-to-I transition temperature and the correlation length; (b) suppression of the N phase manifested in the decrease of the N-to-I transition temperature and in separation of the N phase into a more densely packed N phase or the columnar (C) phase, coexisting with a less condensed I phase. The scenario (b) can be triggered by simply increasing pH (adding NaOH). The effects produced by tetravalent spermine fall mostly into the category (b), but the detail depends on whether this additive is in its salt form or a free base form. The base form causes changes through changes in pH and possible excluded volume effects whereas the salt form might disrupt the structure of SSY aggregates.

1. Introduction

Lyotropic chromonic liquid crystals (LCLCs) represent a broad but poorly studied class of soft matter in which the reversibly self-assembled aggregates form liquid crystalline phases.[1–3] The LCLC molecules have a disk-like or plank-like relatively rigid core with two or more ionic groups at the periphery. The molecules tend to aggregate face-to-face, forming stacks with the ionic solubilizing groups exposed at the aggregate-water interface.[1–3] Within the aggregates, the molecules are associated through noncovalent and thus relatively weak interactions such as π–π attraction. The LCLC mesomorphism is usually observed for molecules with lateral size of the order of 1–3 nm; the typical separation between the adjacent molecules along the stacking direction is about 0.34 nm. With two ionic groups per molecule, the maximum line density of charges is very high, $\tau e \approx 6e$/nm (e is the electron's charge). The stacking distance and the line charge make LCLC aggregates similar to the double-strand B-DNA molecules with the important difference that in LCLCs, there are no covalent bonds to fix the shape and size of the aggregates. The latter can thus be expected to vary strongly with concentration,[1–3] ionic content,[4] temperature,[5] nature of side groups[3,6] and counterions,[3,7] etc. However, the basic properties of LCLCs, including the molecular structure–property relationship, details

of aggregation, role of concentration, temperature, ionic content remain practically unexplored.

Yu and Saupe discovered[4] that the temperatures of phase transitions in one of the LCLC materials, disodium cromoglycate, or DSCG,[8,9] can be changed by adding a monovalent salt (NaCl). These studies have been continued by Kostko et al.[10] who demonstrated that mono- and divalent salts can either increase or decrease the temperature of the transition between the nematic (N) and the isotropic (I) phase. The mechanisms remain unclear; the situation is not helped by the fact that the very structure of the DSCG aggregates (and other LCLCs[11]) is still being debated.[8,9] S. Krishna Prasad et al.[12] explored the effect of NaCl on another LCLC material, disodium salt of 6-hydroxy-5-[(4-sulfophenyl)azo]-2-naphthalenesulfonic acid, also known as Sunset Yellow FCF (SSY) or Edicol. The authors concluded that neither the dimension of the aggregates nor the dynamics associated with them alter significantly with the addition of NaCl and attributed the observed increase of the LCLC viscosity to the salt-induced changes in the hydrogen bonding.[12]

In the present work, we expand the previous studies and explore the effect of various ionic additives on the mesomorphic properties and structure of SSY, Figure 1.[13–20] SSY as an LCLC has been studied by Ormerod,[13] Luoma,[14] and recently, by Horowitz et al.[15] and Edwards et al.[16] The aggregate structure of SSY is somewhat better established than that of DSCG: the stacks of SSY in water have been shown to contain only one molecule in cross-section;[15,16] the molecules are on average perpendicular to the aggregate axis. The underlying mechanism of aggregate self-assembly in LCLCs is similar to the one responsible for worm-like micelles formed by surfactant mol-
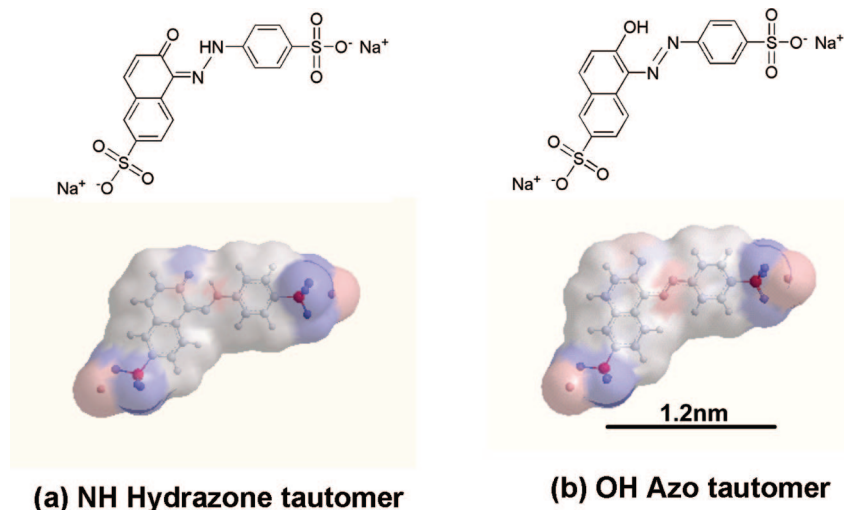
* Corresponding author. E-mail: odl@lci.kent.edu. Fax: 330-672-2796.
† Liquid Crystal Institute and Chemical Physics Interdisciplinary Program, Kent State University.
‡ Department of Physics, Kent State University.
§ Institute of Physical Optics.
|| National Science Foundation.

Figure 1. Molecular structure of two forms of Sunset Yellow FCF, (a) NH hydrazone tautomer and (b) OH azo tautomer. The model structures on the bottom illustrate the relative electric charge distribution: Red color corresponds to the positive charge and blue to the negative charge.

ecules in solutions and the so-called "living" polymerization. The balance of energy gained by placing a monomer inside the aggregate and the entropy term promoting a larger number of aggregates, produces a polydisperse system of linear aggregates (see, e.g., refs 21 and 22) that can arrange into orientationally ordered nematic (N) and columnar (C) phases.[23,24]

By employing optical microscopy and synchrotron X-ray scattering, we explore how the phase diagrams and aggregation in SSY solutions depend on the concentration of SSY and presence of ionic additives such as mono- and divalent salts, tetravalent spermine, and pH-controlling agents. The very existence of N phase in SSY solutions is puzzling, as the correlation length ξ_L measured along the stacking direction in the X-ray experiments, is too small to satisfy the Onsager criterion for orientational order for concentrations at which the N phase is observed. We propose that SSY molecules might form not only the simple rod-like aggregates but also more complex geometries with "stacking faults". We find two universal trends in the additive-induced modification of the N phase. In the first scenario, additives such as mono- and divalent salts enhance the stability of N phase as reflected in the increase of the I−N transition temperature, which can be explained by salt-induced reduction of electrostatic repulsion between the SSY molecules within the aggregates. In the second scenario, additives such as NaOH base, spermine free base or spermine salt, destabilize the N phase: the transition temperatures are decreased and the N phase separates into a more densely packed N phase or C phase, coexisting with a less condensed I phase. One distinct mechanism here is brought about by pH: at higher pH, the SSY molecules acquire a higher negative charge and are less likely to aggregate. Interestingly, a subsequent addition of HCl that reduces pH, stabilizes the N phase, thus reversing the effect of bases. However, other mechanisms, such as electrostatic attraction and excluded volume effects, can also intervene when the additive is spermine, either in its salt or in its free base form.

2. Experimental Techniques

2.1. Materials. The SSY batch used in this investigation was purchased from Sigma Aldrich and had a purity of 95.7%, according to the HPLC test by Sigma Aldrich. The two main types of impurities in SSY are as follow: (a) byproducts of synthesis with molecular structure close to that of SSY, such
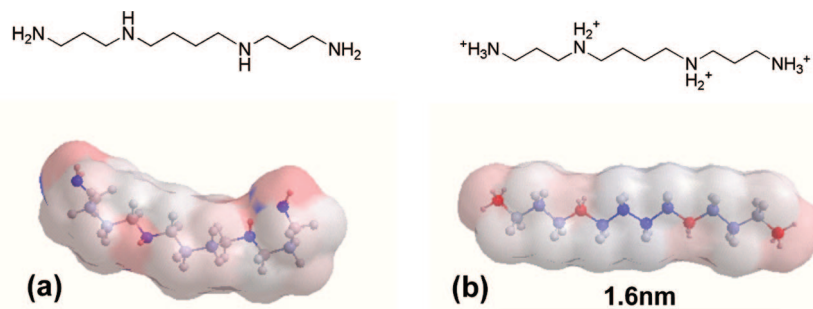
as the trisodium salt of 3-hydroxy-4-(4-sulfophenylazo)-2,7-naphthalenedisulfonic acid and the trisodium salt of 6-hydroxy-7-(4-sulfophenyl)-5-(4-sulfophenylazo)-2-naphthalenesulfonic acid,[25,26] the latter representing a molecule in which an additional sulfophenyl group is attached to the SSY core; (b) lower-molecular weight compounds such as inorganic salts; for example, NaCl is used to induce dye precipitation in the last step of the SSY synthesis. The HPLC-determined number 95.7% specifies mainly that the material contains about 4.3% of impurities (a); it does not provide information on the quantity of (b). To purify SSY from impurities (b), we followed the procedure established earlier.[13−15] Namely, SSY was dissolved in deionized water with the subsequent addition of ethanol to cause precipitation of the dye. The precipitate was filtered from the solvent with impurities (b) and dried in vacuum; the procedure was repeated twice.[13−15] This purification procedure makes our data comparable to those obtained earlier by Ormerod,[13] Luoma,[14] and Horowitz et al.[15] However, we cannot compare our results to those reported in ref 12, as SSY was used in ref 12 as obtained from Aldrich without further purification.

SSY might exist in two tautomeric forms: an NH hydrazone form, Figure 1a, with the hydrogen residing on the distant nitrogen of the azo bond, and an OH azo-tautomer form, with the hydroxide proton residing on the oxygen in ortho to the azo bond, Figure 1b. For most phenylazonaphthols, the NH hydrazone form has been reported as dominating in water solution.[17,18] Edwards et al.[16] demonstrated that the NH hydrazone form, Figure 1a, prevails for both monomers and stacks of SSY.

The sulfonate groups play an important role in water solubility of SSY, as they are easily ionized in the broad range of pH.[19,20] SSY in water is negatively charged, with the molecular charge ∼2e at neutral pH. The negative charge increases with pH,[17] as a result of additional ionization of either OH or N−NH groups in the central part of the SSY molecules.

All additives used were of regent grade, purchased from Sigma-Aldrich, and used without further purification. These are:

(a) mono- and divalent salts: sodium chloride (NaCl), lithium chloride (LiCl), ammonium chloride (NH_4Cl), sodium acetate (CH_3COONa), sodium sulfate (Na_2SO_4), magnesium sulfate ($MgSO_4$);

Self-Assembly of Lyotropic Chromonic LC Sunset Yellow

J. Phys. Chem. B, Vol. 112, No. 51, 2008 **16309**

Figure 2. Molecular structure of spermine in the neutral form (Spm^0) (a) and fully charged form (SpmH$_4^{4+}$) (b).

(b) multivalent agents: spermine tetrahydrochloride salt (Spm·4HCl, abbreviated as SpmCl$_4$), and spermine free base (Spm);

(c) monovalent pH changing agents: sodium hydroxide (NaOH) and hydrochloric acid (HCl).

Spermine free base is a polyprotic base which has four basic sites. It adopts different forms: a neutral Spm^0, single-charged SpmH$^+$, and multiple-charged SpmH$_2^{2+}$, SpmH$_3^{3+}$, and SpmH$_4^{4+}$, Figure 2. The relative concentration of these depends on pH. At low pH, the ammonium groups are more likely to be protonated and thus positively charged. Using the values of the acid dissociation constants (pK_a) for charged forms of spermine from ref 27, we estimated their relative population in water solutions as a function of pH. At pH = 6, Spm molecules are almost completely protonated, and they exist in multivalent ionic forms; more than 99% of them have a charge 4+. As pH increases, the dissociation of these charged protonated forms becomes more likely and Spm becomes less charged; above pH = 11, the predominant form is neutral and fully basic Spm^0.

We use molality units for SSY concentration c, determined as the number of moles of SSY in 1 kg of water, and the volume fraction units, $\phi = cW_{SSY}\rho_{water}/(\rho_{SSY}) + (cW_{SSY}\rho_{water})$. Here W_{SSY} = 0.452 kg/mol and $\rho_{SSY} = 1.4 \times 10^3$ kg/m^3 are the molecular weight and density of SSY,[14] $\rho_{water} = 1.0 \times 10^3$ kg/m^3 is the density of water. We focus on highly concentrated solutions, c = 0.7−1.3 mol/kg.

The phase diagram is sensitive to purity and hydration of SSY. The phase transition temperatures in solutions prepared from the commercially available SSY (used as purchased) are about 6 °C lower than those for SSY purified as specified above. The degree of SSY dehydration prior to preparation of mixtures is an important issue. In all our experiments, SSY was dehydrated by placing it after purification in a vacuum oven for two days. We tested how easily the dry SSY might be hydrated during the storage, by monitoring the weight of three samples (about 0.3 g each), one in an open vial, another one in a vial closed with a plastic lid, and the third one in a vial closed with a plastic lid and sealed with a parafilm. The SSY vials were placed next to an open water beaker (100 g) at room temperature. Over the two days, the open sample of SSY added about 20% to its weight, and SSY in the closed vial gained about 5%. The third sample, with a lid and a parafilm, added only 1% over 1 month of storage. To avoid hydration effects, we placed the purified and dried SSY in a desiccator; the weight gain was only 0.1% over the period of 3 months. In the experiments, we used either freshly prepared samples or the samples in well sealed vials kept in a desiccator.

We prepared the mixtures by adding SSY to water that already contained dissolved additives, to avoid occurrence of accidentally inhomogeneous specimen. Finally, to avoid any

nonspecific effects in the mixtures with additives, we always used a control sample and measured the additives-induced changes in temperatures of phase transitions as a relative change with respect to the temperature $T_{I \to I+N}$ of the I→I+N transition of a control sample (with no additives), prepared with SSY obtained from the same batch, purified and stored the same way as SSY in the samples with additives. This protocol also helped to mitigate the aging effects. We used Millipore water with initial resistivity $\geq$18.1 MΩ·cm in preparation of all solutions.

2.2. Optical Studies of Phase Transitions. Two different techniques were used to prepare the samples for optical observations: (a) by placing a drop of the solution between two glass plates separated by mylar spacers (thickness 6 and 12 μm) and sealing the edges of the cell with an epoxy glue (Davcon) and nail polish and (b) by filling the solutions into a rectangular capillary that is 20 or 40 μm thick and 200 or 400 μm wide and then sealing the ends of the capillary. The phase behavior was determined by observing the samples through a polarizing microscope, while changing the temperature at a rate of 0.2 °C/min.

To explore multiple compositions, we used arrays of capillaries each filled with a different composition, placed into a temperature gradient, Figure 3.[28] The temperature gradient was created by circulating hot and cold water along two tubes at the opposite ends of the arrays, Figure 3. The temperature gradient was calibrated with a thermocouple and adjusted to be practically linear, $T(x) = T_{cold} + (T_{hot} - T_{cold})x/X$, where $T(x)$ is the local temperature at the point x along the capillary axis, T_{cold} and T_{hot} are the temperatures at the two ends of the unit, separated by the distance X. The transition temperatures were determined while decreasing the temperature of the "cold" end and using the polarizing microscope to locate the interface between the phases, Figure 3b.

2.3. Synchrotron X-ray Studies. For X-ray diffraction measurements, the solutions were loaded into 1.5 mm diameter Lindéman capillaries with 10 μm thick walls or in sandwich like cells made with 60 μm thick plates. These were placed in an oven under an in situ magnetic field of strength 2.5 kG. The sample was then exposed to synchrotron X-ray radiation of wavelength 0.7653 Å at station 6-IDB of the Midwestern Collaborative Access Team at the Advanced Photon Source of Argonne National Laboratory. The diffraction patterns were recorded at room temperature (T = 28.4 °C) using a high resolution image plate area detector, MAR345, placed at a distance of 476.0 mm from the samples. The data were calibrated against a silicon standard (NIST 640C). The intensity of the incident beam was controlled using a bank of Cu and Al attenuators. Data accumulation times ranged between 1 and 60 s. The 2D diffraction patterns were analyzed using the software package FIT2D developed by Hammersley et al.[29] The length
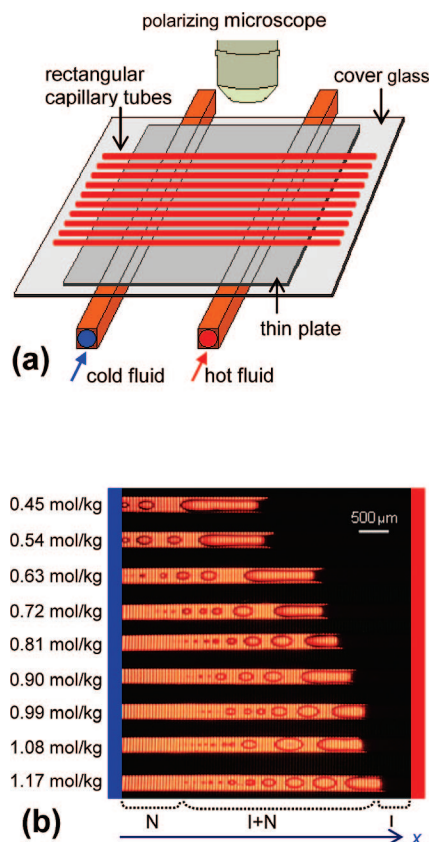
Figure 3. Schematic diagram of the temperature gradient device (a). Polarizing microscopic images allow one to determine the location of the interfaces between the I, N, and biphasic I+N regions, and thus to determine the temperatures of corresponding phase transitions, as illustrated for a $c = 0.9$ mol/kg SSY solution doped with various amounts of salt $MgSO_4$ indicated on the left-hand side in the mol/kg units (b).

scale and the correlation lengths corresponding to various peaks were calculated from the position and width of the diffraction peaks.

3. Experimental Results

3.1. Phase Diagram of Pure SSY in Water. Figure 4 shows the phase diagram and typical textures of the water solutions of SSY. The phase diagram shows I, N and C phases with broad coexistence regions. The N phase produces Schlieren textures with disclinations (characterized by two dark brushes of extinction) and point defects-boojums (with four brushes of extinction).[30] The columnar phase shows characteristic "developable" domains.[30] The phase diagram is in good agreement with Horowitz et al. data[15] (note that the notation for concentrations in ref 15 should read "mol/kg" instead of "M"[31]) and with Edwards et al.[16] We observe the C phase at $c \geq 1.2$ mol/kg, Figure 4, whereas in ref 16, the C phase is observed for $c \geq 1.4$ mol/kg. This discrepancy might be caused by the degree of SSY purification and dehydration, or by a different initial purity of SSY.

The phase identification is confirmed by the X-ray data, Figure 5 and Table 1. The spacing $a_z = 0.33$ nm in the meridional peak corresponds to the average distance between SSY molecules along the aggregation direction. In the I phase, $c = 0.7$ mol/kg, the aggregates have no particular orientation, Figure 5a. The inter-aggregate distance is $D = 3.11$ nm with a correlation length $\xi_D = 4.42$ nm.

The correlation length ξ_L corresponding to the correlated stacking with the period a_z was determined from the half-width

of the X-ray peak to be 2.4 ± 0.2 nm. If one assumes that the aggregates are ideal rods, with SSY molecules stacked on top of each other, and that ξ_L is a measure of an average length L of such a rod-like stack, then the corresponding aggregation number would be $\langle n \rangle_I \approx 7.3$. However, association of ξ_L with L might be an oversimplification, as the aggregates might be larger (longer) than ξ_L. A number of ξ_L units can assemble into an aggregate through "stalking faults" junctions, junctions with lateral molecular shifts, 3-fold junctions, etc., in which the correlations seen in the X-ray data are lost but the physical connectedness is preserved.

Figure 5b shows the X-ray diffraction pattern for a $c = 0.9$ mol/kg N phase in the magnetic field directed horizontally, as indicated by the arrow in Figure 5b. The director $\hat{n}$ aligns perpendicularly to the magnetic field; the walls of the vertical circular capillary containing the sample, being perpendicular to the magnetic field, assist in a uniform alignment of $\hat{n}$ along the axis of the capillary, i.e., vertically. In the aligned N samples, the X-ray reflections along the horizontal direction (and along the magnetic field) are thus associated with the inter-aggregate distance D (which decreases to $D = 2.63$ nm in the N phase). This feature supports the H-aggregation model,[32] with the molecules stacked on top of each other, being on average perpendicular to the aggregate axis and $\hat{n}$. The staking separation $a_z = 0.33$ nm remains the same as in the I phase. The associated correlation length in the N phase is $\xi_L = (3.5 \pm 0.2)$ nm; the aggregation number corresponding to the *correlated stacking* is $\langle n \rangle_N \approx 10.4$. A further increase of c leads to the C phase; the main feature here is a dramatic sharpening of the small angle peak which arises from the long-range hexagonal packing of the columns in the plane perpendicular to $\hat{n}$. The correlation length is high, $\xi_L = 13.4$ nm at $c = 1.36$ mol/kg. The aggregates are packed more tightly, with $D = 2.07$ nm. Table 1 summarizes the X-ray data for four different concentrations of SSY.

3.2. Effect of Monovalent and Divalent Salts. Monovalent salts studied in this work increase the temperature $T_{I \to I+N}$ at which the first nuclei of the N phase appear from the I melt upon cooling. These salts also increase the width of the biphasic I+N region, Figure 6a. For further discussion, we define the salt-induced temperature shifts of the phase transitions with respect to the temperature $T_{I \to I+N}$ of the I→I+N transition determined for the salt-free SSY solutions (see section 2.2). The shift in the I→I+N transition temperature, $\Delta T_{I \to I+N}(c_s) = T_{I \to I+N}(c_s) - T_{I \to I+N}(c_s = 0)$ is positive, about 4–6 °C, for all studied monovalent salts added at molal concentrations $c_s = 0.5$ mol/kg, Figure 6a.

We extended the studies to salts with a divalent cation. In DSCG,[10] divalent salts caused precipitation. In SSY, divalent cations increase $T_{I \to I+N}$, as illustrated in Figure 6b for salts $MgSO_4$ and $MgCl_2$. Quantitatively, the effect of divalent salts is stronger than that of the monovalent salts such as NaCl, as the corresponding values of $\Delta T_{I \to I+N}(c_s)$ are higher. Figure 6b demonstrates the specificity effect of anions. $MgSO_4$ and $MgCl_2$ with the same cation Mg^{2+}, but a different anion, impart different changes: the sulfate anion SO_4^{2-} produces a larger temperature shift $\Delta T_{I \to I+N}(c_s)$ as compared to the Cl^- anion. Note that in the Hoffmeister series for anions, $SO_4^{2-} > HPO_4^{2-} > CH_3COO^- > Cl^-$, so that SO_4^{2-} is more strongly hydrated as compared to Cl^-.

The strong effect of divalent salts is also illustrated by the fact that $MgSO_4$ added with concentration $c_s = 0.54$ mol/kg to the initially isotropic $c = 0.7$ mol/kg SSY solution, causes an appearance of the N phase coexisting with the I phase, Figure 7. In this N phase, $\xi_L \approx 3.4$ nm (a_z remains equal 0.33 nm),
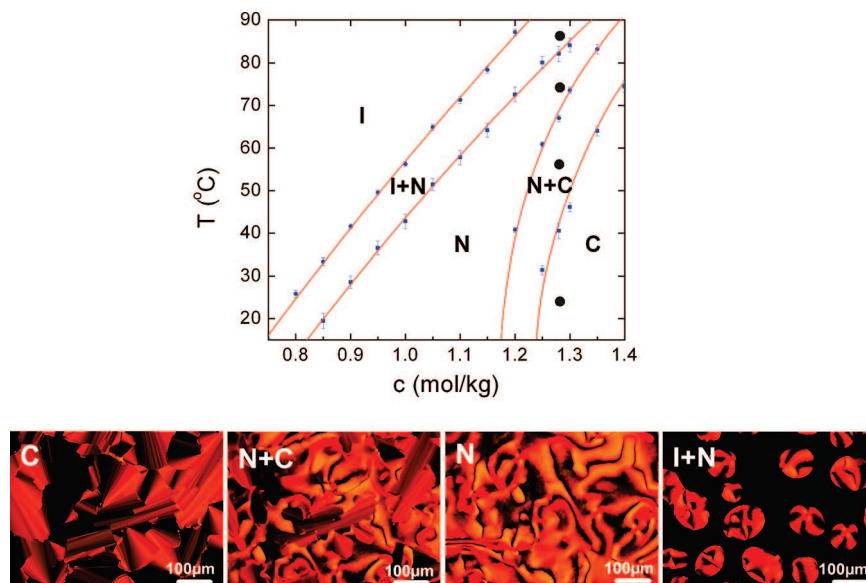
Figure 4. Phase diagram and polarizing microscope textures of SSY water solutions. The error bars represent the difference between the data taken on heating (upper end of the bar) and cooling (lower end of the bar). The filled circles at the vertical line indicate the temperatures at which the textures were taken.
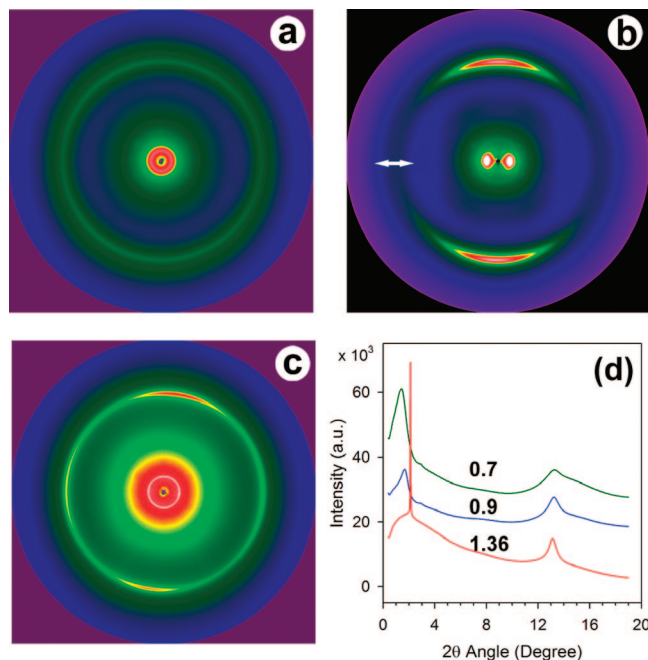
Figure 5. Typical X-ray patterns (a)−(c) and diffractographs (d) of SSY water solutions at different concentrations c: (a) I phase, $c = 0.7$ mol/kg; (b) N phase, $c = 0.9$ mol/kg solution; (c) C phase, $c = 1.36$ mol/kg. All data are taken at 28.4 °C. The three graphs in (d) correspond to the same concentrations c: 0.7 mol/kg (green), 0.9 mol/kg (blue), and 1.36 mol/kg (red).

TABLE 1: Inter-aggregate Axis-to-Axis Distance D, Corresponding Correlation Length ξ_D, Correlation Length ξ_L along the Stacking Direction for Four Different Concentrations of SSY in Water, Expressed in Molal c and Volume Fraction ϕ Units[a]

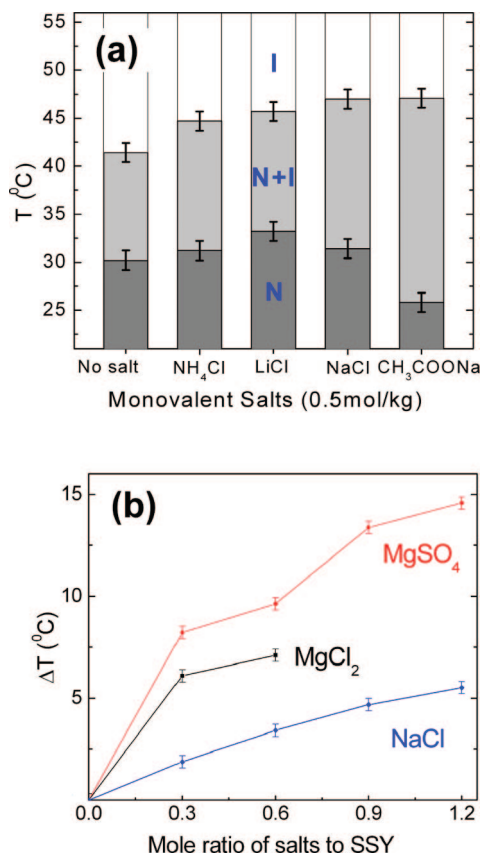| phase	I	N	N	C
c (mol/kg)	0.7	0.9	1.14	1.36
ϕ	0.184	0.225	0.269	0.305
D (nm)	3.11 ± 0.03	2.63 ± 0.02	2.34 ± 0.02	2.07 ± 0.01
ξ_D (nm)	4.42	5.56	8.56	104.72
ξ_L (nm)	2.4 ± 0.2	3.5 ± 0.2	4.8 ± 0.2	13.4 ± 0.2

[a] The temperature is fixed at 28.4 °C.

distance, $\xi_L \approx 4.0$ nm. This values is somewhat larger than $\xi_L \approx 3.5$ nm for $c = 0.9$ mol/kg SSY solution with no salt, Figure 5b,d. Although ξ_L increases and the aggregates are closer to each other in the doped N phase as compared to the unsalted N phase, the material remains in the homogeneous N phase; we see no signs of coexisting I phase, neither in optical nor in X-ray features at 28.4 °C. Addition of MgSO$_4$ increases the temperatures of both I→I+N and I+N→N transitions. Among the possible explanations might be the following: (a) the structure of SSY aggregates is more complex than the simple rods so that ξ_L is the scale of a locally correlated assembly of the monomers rather than the size of the entire aggregate; (b) the salt alters the size distribution of aggregates.

3.3. Effects of Spermine in a Salt and Free Base form. Adding Spm in its salt form SpmCl$_4$ or in the free base form leads to effects that are in some sense opposite to that caused by mono and divalent salts. Namely, the main effect, at least when small amount of Spm ($c_{spm} < 0.1$ mol/kg) is added, is in the decrease of the temperatures of both I→I+N and N+I→N transitions; the biphasic I+N region widens up, Figure 8. At higher concentrations, the nature of changes depends on the form of Spm and on the initial concentration of SSY.

The multivalent salt SpmCl$_4$ added to the $c = 1.14$ mol/kg water solution of SSY in the N phase in the broad range of concentrations, $c_{spm-s} = (0.1-0.7)$ mol/kg, decreases the temperatures of both I→I+N and I+N→N phase transitions and widens up the biphasic I+N region, Figure 8a.

i.e., practically the same as for the N phase of the unsalted $c = 0.9$ mol/kg SSY solution, and larger than $\xi_L \approx 2.4$ nm measured in the unsalted SSY solution at $c = 0.7$ mol/kg (all data are taken at 28.4 °C). In the salt-condensed N phase of the biphasic region, the aggregates are also packed more tightly as compared to the original I phase: $D = 2.9$ nm, $\xi_D = 3.6$ nm.

X-ray data for a more concentrated solution, $c = 0.9$ mol/kg, doped with $c_s = 0.54$ mol/kg of MgSO$_4$, are shown in Figure 7c,d. In Figure 7c, it is clear that the second peak for $c = 0.9$ mol/kg solution is sharper than that for $c = 0.7$ mol/kg. From the shape of the second peak in Figure 7c, we calculate the correlation length associated with the $a_z = 0.33$ nm repeat

Figure 6. Effect of salts on transition temperatures in $c = 0.9$ mol/kg SSY water solution: (a) I→(I+N) and (N+I)→N transition temperatures in presence of monovalent salts at $c_s = 0.5$ mol/kg for 0.9 mol/kg SSY solution; (b) I→(I+N) transition temperature shift $\Delta T_{I \to I+N}(c_s)$ caused by salts with a divalent cation, data with monovalent salt NaCl are shown for comparison.

The effect of Spm in its *free base* form also starts from the decrease of the transition temperatures. For example, addition of Spm with $c_{spm-b} = 0.3$ mol/kg to $c = 0.9$ mol/kg of SSY solution kept at 28.4 °C, transforms the homogeneous N phase into a homogeneous I phase; ξ_L reduces from 3.5 nm to merely 2.4 nm. In more concentrated SSY solutions, the effect is more dramatic: Spm free base separates the homogeneous N phase into the coexisting C and I phase, Figure 8b. The C inclusions have hexagonal shape and develop "petal" morphology[33] when the columns are perpendicular to the bounding plates, Figure 8b. The hexagonal order of the C phase is confirmed by the X-ray data, Figure 9a,b. In the three-component mixture with $c = 1.14$ mol/kg of SSY and $c_{spm-b} = 0.3$ mol/kg of Spm free base, one observes the coexisting I and C phases, with two inter-aggregate distances, $D = 2.46$ nm and $D = 2.0$ nm, respectively. In the pure SSY solution (no Spm) at $c = 1.14$ mol/kg, this distance is intermediate, $D = 2.34$ nm, and the material forms a homogeneous N phase.

As seen in Figure 8b, adding a moderate amount, $c_{spm-b} \sim 0.1$ mol/kg of Spm free base to the homogeneous N phase causes its separation into N and I phase. In the "condensed" N phase, the aggregates are closer to each other than in the original homogeneous N phase, Figure 9c (although one observes a small increase in D at $c_{spm-b} = 0.05$ mol/kg, Figure 9c). At higher c_{spm-b}, when the condensed state is in the hexagonal C phase, D decreases, Figure 9c. However, the aggregates do not contact each other. According to refs 15 and 16, there is just one molecule in the cross-section of a SSY aggregate; its diameter d is in the range from 1 nm[13,16] to 1.4 nm.[14] Comparing D in
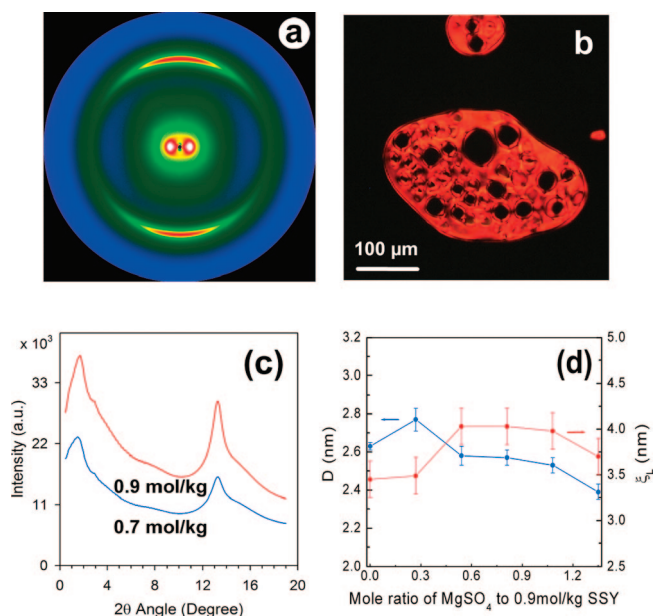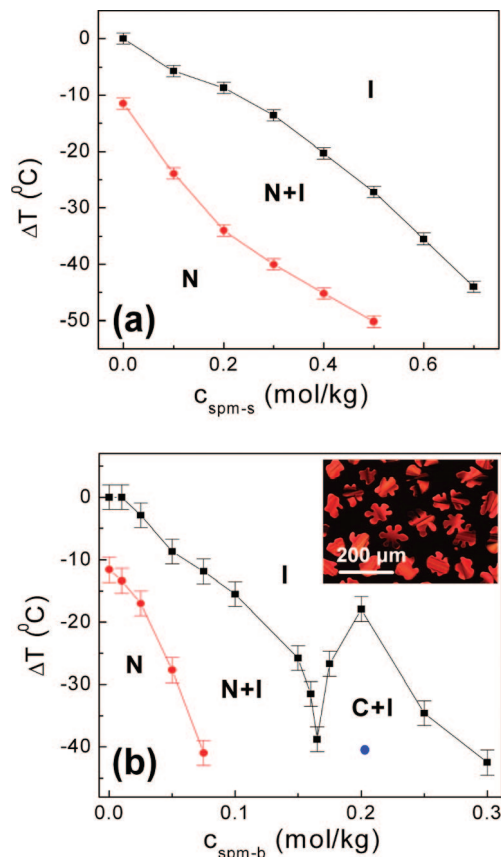

Figure 7. X-ray diffraction pattern (a) and polarizing-microscope texture (b) of the N phase induced by adding $c_s = 0.54$ mol/kg of MgSO$_4$ to the I phase of $c = 0.7$ mol/kg water solution of SSY. (c) Diffractographs for $c = 0.7$ mol/kg and $c = 0.9$ mol/kg water solutions of SSY, both doped with $c_s = 0.54$ mol/kg of MgSO$_4$. (d) Inter-aggregate distance D and correlation length ξ_L of $c = 0.9$ mol/kg SSY solution with increasing concentration c_s of MgSO$_4$. Four diffuse spots in the outer region of the inner green area also appear and are responsible for the third weak reflection shown near 8° (corresponding to spacing of approximately 0.56 nm). All data are taken at 28.4 °C.

Figure 9c and *d*, one concludes that the lateral surfaces of aggregates are separated by the distance $\Delta = D - d$ that is relatively large, $\Delta = 0.8 - 1.3$ nm in the condensed N phase and $0.6 - 1.1$ nm in the C phase. Therefore, the attractive forces triggered by Spm free base are balanced at some equilibrium D by a short-range repulsion.

By adding Spm in its free base form, one inevitably changes the pH of the SSY solution. For example, we determined experimentally using a pH meter (UB-10, Denver Instrument) that addition of $c_{spm-b} = 0.2$ mol/kg of Spm free base to $c = 1.14$ mol/kg SSY water solution increases pH from 6.49 to 11.33. For comparison, pH = 12.01 for $c_{spm-b} = 0.2$ mol/kg water solution of Spm free base with no SSY and pH = 6.08 for 1.14 mol/kg SSY doped with $c_{spm-s} = 0.2$ mol/kg of salt SpmCl$_4$. At elevated pH, as already indicated, Spm transforms into the mostly neutral form Spm^0, whereas SSY molecules at high pH increase their negative charge.[17,19] We observe that pH can dramatically alter the changes introduced by Spm free base in SSY phase diagram. Namely, by adding the acid HCl to a mixture of SSY, Spm free base and water (in which Spm has already caused a biphasic I+C state), and thus decreasing pH, one restores the homogeneous N phase and reverses the phase separation effect caused by Spm free base, Figures 10 and 11. This experiment demonstrates not only that pH and the state in which Spm exists in the solution are important; it also underlines that high concentrations of Spm free base that condense the SSY aggregates into the C phase do not change irreversibly the structure of these aggregates.

3.4. Effects of Monovalent pH Changing Agents. A simple pH-increasing agent, NaOH base, produces an effect similar to Spm free base. NaOH was added to $c = 1.14$ mol/kg SSY solution. At low concentrations ($c_{NaOH} < 0.1$ mol/kg), NaOH reduces the transition temperatures of the I→I+N and N+I→N

Self-Assembly of Lyotropic Chromonic LC Sunset Yellow

J. Phys. Chem. B, Vol. 112, No. 51, 2008 **16313**

**Figure 8.** Phase diagrams of $c = 1.14$ mol/kg SSY solution doped with the salt $SpmCl_4$ (a) and Spm free base (b); the inset shows the polarizing microscope texture of the I+C biphasic region corresponding to the blue circle at the phase diagram.

transitions. At higher concentrations, NaOH produces first a biphasic region N+I ($c_{NaOH} = 0.1$ mol/kg) and C+I ($c_{NaOH} = 0.2$ mol/kg), then a completely homogeneous I phase and finally, a crystalline precipitate, Figure 12. The changes introduced by NaOH are qualitatively similar to the changes caused by Spm free base, Figure 8b and are in a marked contrast to the stabilizing effect of the monovalent salts such as NaCl on the N phase, Figure 6. By adding the acid HCl to the solutions of SSY with NaOH, and thus reducing pH, one effectively reverses the effect of NaOH, restoring the N phase with somewhat higher temperatures of phase transitions. The later is easy to understand, as simultaneous presence of NaOH and HCl is equivalent to adding a salt NaCl to the SSY solution that is promoting the N phase.

4. Discussion

Aggregation and subsequent self-assembly of SSY molecules into the N and C phases depends on a number of factors. (A) The intra-aggregate interactions responsible for the monomer stacking and reversible aggregation, are determined mainly by (A1) noncovalent attractive forces such as $\pi-\pi$ interaction and (A2) repulsive electrostatic forces between the ionized groups, such as sulfonate groups. The extent of ionization of these groups depends on the relative acidity or basicity (pH) of the solvent. (B) The inter-aggregate interactions are mainly controlled by (B1) excluded volume effects, as in the Onsager model of nematic order;[34] (B2) (screened) electrostatic forces, usually of a repulsive nature; dynamic and static fluctuations in local concentrations of differently charged species might also cause attractive electrostatic forces between similarly charged ag-
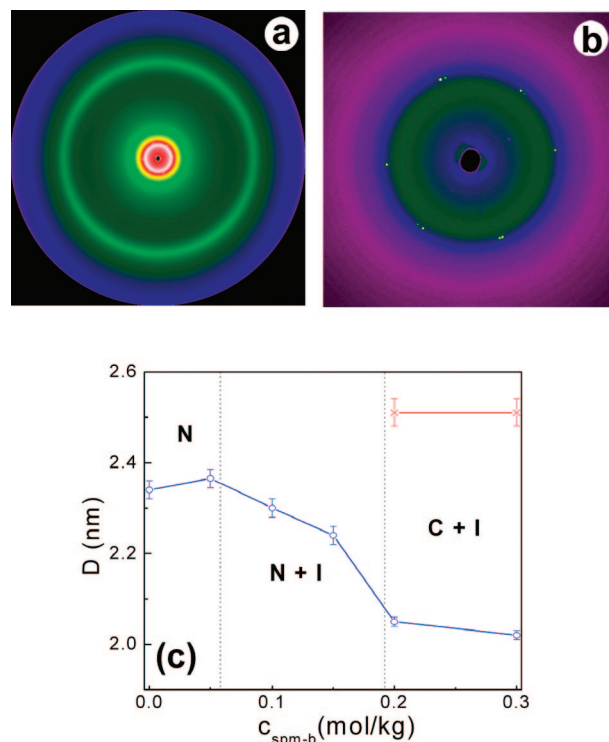
Figure 9. X-ray diffraction patterns, (a) wide angle and (b) small angle range, of the coexisting I and C phases in the $c = 1.14$ mol/kg SSY water solution doped with $c_{spm-b} = 0.3$ mol/kg of Spm free base. Note hexagonal symmetry in part (b). (c) Inter-aggregate distance D vs Spm concentration for the condensed birefringence regions (o) and for the I phase (×). All data are taken at 28.4 °C.
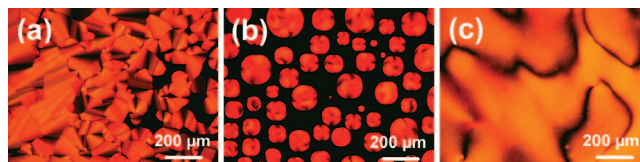
Figure 10. Polarizing microscopy textures illustrating a transformation of a biphasic I+C state of a water solution with $c = 1.14$ mol/kg SSY and $c_{spm-b} = 0.2$ mol/kg Spm free base into a N phase upon addition of HCl in concentrations 0.008 mol/kg (a), 0.04 mol/kg (b), and 0.4 mol/kg (c). The textures show (a) C phase coexisting with I phase. (b) N droplets surrounded by I phase and (c) Schlieren texture of a homogeneous N phase. All textures are taken at 25 °C.

gregates, (B3) repulsive hydration forces (i.e., forces derived from the work needed to dehydrate the hydrophilic lateral surfaces of the aggregates, see, e.g., refs 35 and 36).

4.1. Additive-Free SSY Solutions in Water. In the absence of any additives such as salt, the simplest phenomenological model to describe the phase diagram of SSY in water can be based on the enthalpy–entropy balance of reversible self-assembly of one-dimensional aggregates, similar to the models of worm-like micelles or "living" polymers.[21,22] The monomers, in our case disk-like SSY molecules of diameter $d \approx 1$ nm and "thickness" $a_z \approx 0.33$ nm, prefer to stack face-to-face to minimize the areas of unfavorable contact with water. The aggregate would grow indefinitely if it were not for the entropy that is roughly proportional to the number of aggregates. The balance of the "end" energy E_1 of an aggregate (also called the scission energy, i.e., the energy needed to cut an aggregate into two), and the entropy gained by producing more "ends", results in a broadly polydisperse system of rod-like aggregates with the average aggregation number:

$$\langle n \rangle = \sqrt{\phi} \exp \frac{E_1}{2k_B T} \qquad (1)$$

determined by the volume fraction ϕ of the solute and strongly dependent on E_1 and the absolute temperature T; see, e.g., refs 21 and 22.

The relationship (1) has been derived for dilute *isotropic* solutions and for electrically *neutral* monomers; the later assumption does not apply to SSY. The ionic groups of SSY dissociate in water, producing electric charges at the lateral surface of aggregates and releasing Na^+ counterions. Mutual Coulomb repulsion weakens the association of monomers and reduces the scission energy $\tilde{E}_1 \rightarrow E_1 - E_e$. The electrostatic correction E_e should depend on spatial distribution of the counterions and ϕ.

For highly charged linear aggregates, some of the counterions are immobilized at the surface[38–42] and some are released into the solvent. The condensed counterions decrease the effective charge of the rod from the maximum possible $\tau e \approx 6e/nm$ to $\tilde{\tau}e \sim e/l_B$, where $l_B = e^2/4\pi\varepsilon\varepsilon_0 k_B T$ is the Bjerrum length, i.e., the distance at which the repulsion energy of two elementary charges e equals the thermal energy $k_B T$. For water at room temperature, $l_B \approx 0.7$ nm and thus $\tilde{\tau}e \approx 1.4e/nm$. Furthermore, E_e should decrease with ϕ: as ϕ increases, the clouds of "free" counterions are pushed closer to the aggregates and thus screen more effectively the charges of monomers in them (each elementary cell comprising an aggregate with the surrounding counterions should be electrically neutral).[37] For moderate $\phi \leq 0.1$, MacKintosh et al.[37] found that the aggregation number for one-dimensional aggregates in an isotropic solution is modified as:

$$\langle n \rangle = \sqrt{\phi} \exp \frac{E_1 - E_e}{2k_B T} \qquad (2)$$

where $E_e = l_B d\tilde{\tau}^2 k_B T/2\phi^{1/2}$. In the order of magnitude, $E_e \approx 1.7k_B T$ for $\phi = 0.18$ (which corresponds to the I phase at room temperature).

If one assumes the rod-like model of SSY aggregates, then the experimental value $\xi_L = 2.4$ nm in the I phase can be used to determine $E_1 - E_e$ from eq 2, as the aggregation number $\langle n \rangle \approx \xi_L/a_z \approx 7.3$ is known in this model. One estimates $E_1 - E_e \approx 5.7k_B T$ and $E_1 \approx 7.4k_B T$, close to the values reported by Luoma[14] and Horowitz et al.[15] for SSY and by Nakata et al.[43] for a similar self-assembling system of short DNA segments. Importantly, E_e is significant as compared to E_1; changes in the electric charges of monomers, either through electrostatic screening or through pH-induced modifications, can greatly influence the aggregation described by eq 2.

According to eq 2, a higher ϕ should facilitate aggregation, in qualitative agreement with our experiments, Table 1. When the length-to-diameter ratio L/d of the rod-like aggregates and ϕ are sufficiently high, the solution should experience I→N phase transition, according to the Onsager theory.[34] A *monodisperse* system of rigid neutral rods forms N phase when ϕ exceeds a critical value $\phi_{IN} \approx 4d/L$.[34,44,45] This condition cannot be fulfilled in our experiments if we treat the structure of SSY aggregates as straight rods. In our experiments, the N phase clearly exists at $\phi \approx 0.23$ when $\xi_L \approx 3.5$ nm, Table 1. If one identifies the correlation length ξ_L with L and takes $d = 1$ nm, then $L/d \approx 3.5$ and $\phi L/d \approx 0.7$, clearly too small as compared to $\phi_{IN}L/d \approx 4$ to fulfill the condition for the N order. Numerical
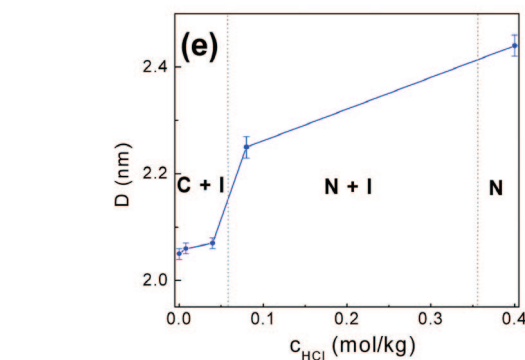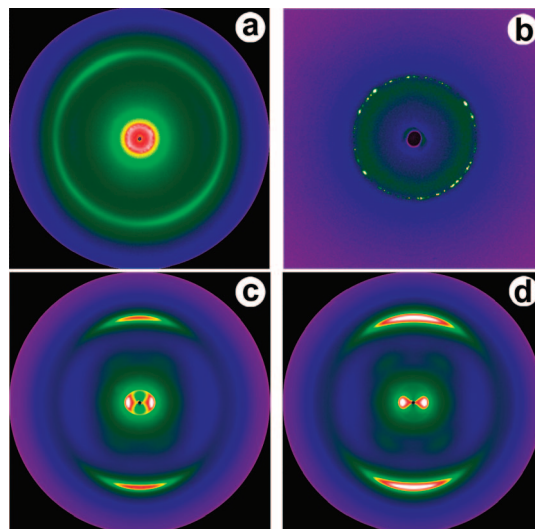
Figure 11. X-ray diffraction patterns illustrating a transformation of a biphasic I+C state of a water solution with $c = 1.14$ mol/kg SSY and $c_{spm-b} = 0.2$ mol/kg Spm free base into a N phase upon addition of acid HCl. The diffraction patterns for the mixture with no HCl added, recorded at large (a) and small (b) angles. The diffuse (green) rings at large and small angles and sharp reflections at small angle indicate a coexistence of I and C phases. When 0.08 mol/kg (c) and 0.4 mol/kg (d) of HCl are added, the diffraction patterns show the N phase well aligned by the in situ magnetic field. The length scales corresponding to the small angle (horizontal) and wide angle (vertical) reflections in (c) and (d) are 22.5/24.4 Å and 3.33/3.33 Å. There are four faint reflections visible at approximately 5.6 Å, which may be due to the phenyl group of these molecules being oblique to the nepthalene plane of the hydrazone form of SSY or to other effects, such as formation of chiral arrangements of dye molecules within the aggregates, etc. Equal numbers of phenyl groups appear to be pointing up and down at ∼36° relative to the aggregate axis. (e) Inter-aggregate distance D in the condensed liquid crystalline phases of $c = 1.14$ mol/kg SSY and $c_{spm-b} = 0.2$ mol/kg Spm solution vs the concentration of added acid HCl. All data are taken at $T = 28.4$ °C.

simulations[44] demonstrate that there should be no orientational order in the Onsager system at any ϕ, if $L/d < 4.7$. In other words, from the point of view of the Onsager model, the N phase of rod-like aggregates in our solution with $\phi \approx 0.23$, $d \approx 1$ nm, and $L \approx \xi_L \approx 3.5$ nm should not exist.

In the estimates above, we used the minimum "bare" value of d, as if the aggregates were electrically neutral. Accounting for the effect of charges here would not improve the situation. Mean-field theories[34,46] predict that electric charges in rod-like polyelectrolyte solutions cause Coulomb repulsion of similarly charged rods and thus favor perpendicular alignment (a "twist" effect), which amounts to destabilization of the N phase. Potemkin et al.[47,48] considered the many-body Coulomb interactions in salt-free polyelectrolyte solution and concluded that
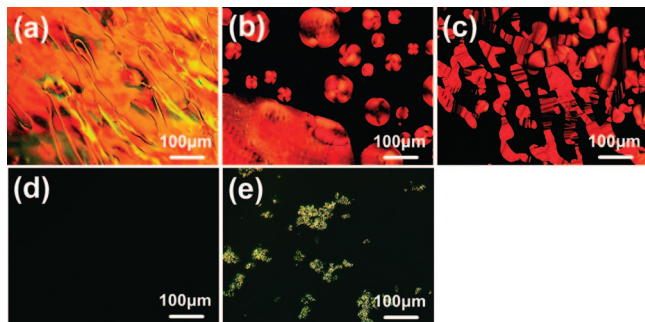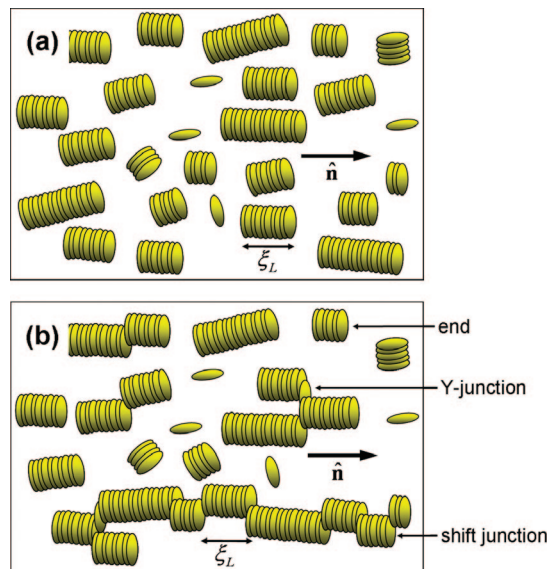
Figure 12. Polarizing microscopy textures for $c = 1.14$ mol/kg SSY solution doped with NaOH at different concentrations: (a) $c_{NaOH} = 0$, pH = 6.5, homogeneous N phase; (b) $c_{NaOH} = 0.1$ mol/kg, pH = 11.6, coexisting N and I phases; (c) $c_{NaOH} = 0.2$ mol/kg, pH = 11.9, coexisting C and I phases; (d) $c_{NaOH} = 0.5$ mol/kg, pH = 12.5, homogeneous I phase; (e) $c_{NaOH} = 2$ mol/kg, pH = 13.2, precipitate. All textures are taken at $T = 25$ °C.

Figure 13. Schematic models of the N phase in a LCLC: (a) a standard model with rod-like aggregates; (b) a model with shift junctions and Y junctions and their clusters, coexisting with the rod-like aggregates.

these interactions might be attractive, thus stabilizing a weakly ordered N phase at very low concentrations of the polyelectrolyte. However, the theory[47] deals with relatively large monomers (larger than $4\pi l_B$) and the predicted N phase exists at concentrations much smaller than $\phi = 0.2$. Besides, the Coulomb attraction and thus the weakly ordered N phase should be suppressed by adding a salt,[48] whereas in our experiments, the salts stabilize the N phase. Taking into account that the aggregates are flexible would not be helpful either in the resolution of the puzzle of small $\phi L/d \approx 0.7$, as flexible rods need an even higher ϕ to produce N phase as compared to their rigid counterparts.[49−52]

The discrepancy between the experimental fact of the existence of the N phase and the smallness of ξ_L might simply indicate that the Onsager theory is not applicable to self-assembled polydisperse aggregates. Indeed, in the Onsager model, the rods are rigid and monodisperse, the phase transitions depend on ϕ but not on T, etc. In LCLCs, the rods are reversibly self-assembled, polydisperse, with T-dependent size;[5] the phase diagram is also T-dependent, Figure 4. In a polydisperse system, the population of longer rods might dictate the onset of the N order, whereas the shorter rods remain disoriented.[50] An approach based on these ideas and thus better fitting the behavior of LCLCs has been proposed by Taylor and Herzfeld.[23] Their model deals with electrically neutral monomers that reversibly self-assemble into one-dimensional rod-like aggregates. The inter-aggregate potential is taken in ref 23 as an infinite hard-core repulsion surrounded by a short-ranged "soft" repulsion of a finite amplitude and width that mimics electric double layers, hydration forces, etc. The total free energy density contains also an ideal mixing term and an intra-aggregate association term with temperature-dependent end energy.[23]

Numerical minimization[23] yields a phase diagram that is qualitatively close to the experimental Figure 4. Namely, the only stable phase at low ϕ is the I phase. Increasing ϕ at $T = $ const, one finds the N and C phases. Both melt into the I phase as T increases (at $\phi =$ const). The two transition lines separating the biphasic I+N region from the homogeneous I and N phases, are tilted with respect to both T and ϕ axes. At high T, there is no N phase but the C phase is preserved. The N−C transition is mostly concentration-driven, and depends little on T. All these features are reproduced in the experiment, Figure 4, indicating that the excluded volume effects and sufficiently large E_1 are the two important features responsible for the formation of LC phases.

However, there are still significant quantitative differences. The model[23] deals with *spherical* monomers and predicts that the aggregation number $\langle n \rangle \approx 10$ at the I−N transition for $\phi \approx 0.2$, which translates into the aspect ratio $L/d \approx 2\langle n \rangle/3 \approx 7$ and $\phi L/d \approx 1.4$.[23] In our experiments, because the SSY monomers are *disk*-like, the same $\langle n \rangle \approx 10$ implies a smaller $L/d \approx 0.33\langle n \rangle \approx 3.3$ and $\phi L/d \approx 0.7$, still below the limit necessary for the formation of the N phase in ref 23.

The source of discrepancies between our experiments and the theoretical models, either the classic Onsager theory[34,44,45] or its modification for reversibly self-assembled monomers,[23,52] appears to be in the oversimplification of the actual shape of aggregates and in the assumption that the correlation length ξ_L reflects the true dimension of the aggregates. We propose that the SSY aggregates can form morphologies more complex than simple rods, with two spatial scales: a short scale ξ_L related to correlated stacking of monomers, and a larger scale characterizing the entire aggregate, composed of connected (but uncorrelated from the point of view of X-ray) ξ_L-branches. The correlation between the ξ_L-branches is lost through "stalking faults" such as molecular lateral shifts, 3-fold "Y" junctions, etc., Figure 13. Note that the Y junctions have been observed in isotropic solutions of block copolymers and surfactants;[53,54] in dry films formed from LCLCs, the Y junctions are seen as prevailing over the open-ended rod-like bundles.[55]

The aggregates should be understood as transient rather than rigid formations. At this stage, it is difficult to describe their detailed geometry. As clear from the molecular structure, Figure 1, an ideal "face-to-face" stacking of SSY molecules is impossible from the electrostatic point of view. The neighboring molecules should shift and rotate with respect to each other, to overlap effectively the electronegative and electropositive regions. The interaction potential landscape, besides the absolute minimum corresponding to the regular stacking, contains local minima for nonideal configurations with a different shift, twist, or a number of immediate neighbors. The occurrence of "defects" or "stacking faults" is facilitated by the existence of two tautomers of SSY, Figure 1, and, clearly, by the presence of impurities of type (a) discussed in section 2.1, representing molecules similar to SSY. All these defects are expected to

increase the configurational entropy of the system. Note that although the Y-junctions might be a universal type of defects in worm-like micelles, living polymers,[56] and LCLCs, the shift stacking faults in Figure 13 appear to be specific to the chromonic aggregation.

Complex geometry of aggregation can reconcile the observed stability of the LC phases with the low ξ_L. Two rod-like branches of length ξ_L linked trough a shift by, e.g., $d/2$, would produce a cluster with an aspect ratio $\sim 2\xi_L/1.5d$, higher than the aspect ratio ξ_L/d of the individual branch. At higher levels of aggregation, with $N \gg 1$ generations of connected branches, one would expect the length of the aggregate to scale as $L_{cluster} \propto N\xi_L$ and the width as $d_{cluster} \propto \sqrt{N}$, as in one-dimensional random walk, so that the aspect ratio increases with N, $L_{cluster}/d_{cluster} \propto \sqrt{N}$. The clusters formed by connected ξ_L-branches would thus be capable to satisfy the Onsager criterion even if the correlation length ξ_L is not.

The phase behavior of the SSY solution even in the absence of additives remains a complex problem. A theoretical model of aggregation that would account for the local minima in the interaction potential and multiple scales of structural organization is clearly in order here. Such a model should explicitly account for the scission energies associated with various types of defects, different from E_1 in eqs 1 and 2.

4.2. Mono- and Divalent Salts. Experimentally, mono- and divalent salts increase the temperature of the N−I transition and even cause the appearance of N phase from an initially isotropic solution, Figure 7. In this salt-induced N phase, ξ_L is larger than in the unsalted isotropic solution.

The aggregated SSY molecules leave the charged sulfonate groups at the aggregate−water interface and can be thus viewed as macroions surrounded by counterions (cations Na$^+$). The sulfonate groups contribute to intra-aggregate electrostatic repulsion and to (screened) inter-aggregate repulsion. Adding salts decreases the Debye screening length $\lambda_D = (1/e)(\varepsilon\varepsilon_0 k_B T/\sum_i c_{si}q_i^2)^{1/2}$ and thus decreases the range of "soft" repulsion. Here ε_0 is the electric constant, ε is the dielectric constant of water, and q is the ion's valency. For SSY, λ_D is determined by (a) the "proper" counterions Na$^+$, two per each SSY molecule; (b) the coions and counterions that come from the added salts. For example, for 300 mM concentrations of 1:1 salt such as LiCl or NaCl, and 1.1 M concentration of SSY, one estimates $\sum_i c_{si}q_i^2 = 2c_{SSY} + 2c_s \approx 2.8$ M and thus $\lambda_D = 0.25$ nm. For a salt 2:1, $q = 2$, such as MgCl$_2$, at the same concentration, one finds $\sum_i c_{si}q_i^2 = 2c_{SSY} + q^2 c_s + qc_s \approx 4$ M and $\lambda_D = 0.21$ nm. The changes in λ_D induced by the salts are relatively small as compared to the "bare" d and D and are not likely to influence the phase diagrams through modification of these geometrical parameters. On the other hand, the salts might affect intra-aggregate interactions, i.e., altering the scission energy and the depth of local minima responsible for "stacking faults". Variations in these could lead to dramatic changes in aggregation size, as the typical dependencies are exponential, eqs 1 and 2.

The salts screen the electric charges of the monomers within the aggregates and thus favor longer aggregates, effectively reversing the trend induced by the electric charges of the monomers themselves in eq 2. As discussed by MacKintosh et al.[37] for cylindrical rods in isotropic solutions, addition of salt is effectively equivalent to the increase of ϕ, thus promoting aggregation. The effect is in qualitative agreement with the experimentally observed increase of the N−I transition temperature in the presence of monovalent and divalent salts. Salt-induced axial growth is known for the wormlike micelles formed by ionic surfactants.[57,58] An increase of the aggregation number

upon the addition of NaCl has been indicated by Edwards et al.[3] However, the complete picture remains unclear, as the relationship between ξ_L and the overall size of the aggregate is not known.

To conclude this section, we note that the MgSO$_4$-induced condensation of the isotropic solution of SSY with $c = 0.7$ mol/kg into a N phase coexisting with the I phase might reflect not only a higher degree of aggregation in the presence of salts but also correlation-mediated electrostatic attractions of aggregates. Typically, the electrostatic attraction of similarly charged rods is observed in the presence of counterions of valency higher than 2, but Qiu et al.[59] demonstrated recently that the attraction of the similarly charged DNA strands can be caused by the divalent Mg^{2+} counterions.

4.3. Multivalent Salt SpmCl$_4$. SSY aggregates with fully dissociated ionic groups are highly charged. The charge density per unit length, $\tau e \simeq 2e/0.33$ nm $= 6$ e/nm is the same as that for the B-DNA. This similarity was one of the factors that stimulated our studies of ionic effects in LCLCs. It is well-known that the electrostatics of highly charged rods leads to a number of fascinating effects, such as "condensation" of DNA, i.e., attraction of the two similarly charged DNA molecules, in the presence of multivalent ions.[59−67] The leading cause of this unusual effect appears to be electrostatic correlations, but the concrete mechanisms remain elusive. Among the possible models, one finds (1) a transient bridging, when a multivalent counterion such as spermine connects two neighboring DNA rods,[63] and (2) formation of patchy regions of counterions condensed at the rods.[40,42,60,62,64] If either model of electrostatic attraction of similarly charged rods were applicable to the case of SSY, the most likely candidate would be a mixture with an added spermine salt SpmCl$_4$. In these solutions, pH remains low, about 6.1 (because of the presence of HCl), so most of the Spm molecules are highly charged, $q = 4$. The charged counterion Spm^{4+}, being relatively long, Figure 2, can directly bridge the neighboring SSY aggregates. Molecular dynamics simulations of Spm find that its mean end-to-end distance is about 1.2 nm.[63] Experimentally, $\Delta = D - d \approx 0.8$−1.3 nm in the N phase and 0.6−1.1 nm in the C phase, so that the Spm^{4+} can in principle bridge the neighboring SSY aggregates, serving as "linkers". This might lead to interesting effects described by Borukhov et al.[68] for linker-assisted filament aggregation, such as formation of macroscopic bundles or transformation of the N phase into coexisting I and C phases. The latter effect is indeed observed in our system, but only when Spm is added in the free base form, Figure 8b, which is likely acting through a different mechanism of the excluded volume.

The condition for attraction through electrostatic correlations without bridging can be written as $\Delta < \Delta_z$, where Δ_z is the distance between the absorbed counterions at the aggregate surface.[42] To estimate Δ_z, let us assume that the adsorbed counterions completely neutralize the charge at the aggregate surface. The condition of electro-neutrality $\Delta_z = q/\tau$ then leads to $\Delta_z = 0.67$ nm for Spm^{4+}, which is smaller than the typical Δ in our experiments. The finite extension of the Spm^{4+} counterions might reduce Δ to favor the electrostatic attraction, but on the other hand, it also implies a departure from the "point-like" picture of the +4 charge needed to maintain a large Δ_z. Therefore, the qualitative considerations cannot unambiguously answer the question whether or not the multivalent ions can cause an electrostatic attraction between the SSY aggregates.

The experiment, on the other hand, shows no significant "condensation" of SSY, at least for $\phi \geq 0.2$ when the system is already in the N phase. The effect of added SpmCl$_4$ is mostly

Self-Assembly of Lyotropic Chromonic LC Sunset Yellow

J. Phys. Chem. B, Vol. 112, No. 51, 2008 **16317**

in suppression of the N phase, Figure 8a. This is in a marked contrast to the situation with DNA, which would condense at a moderate pH in the presence of SpmCl$_4$.[65−67]

It appears that the strongest effect of SpmCl$_4$ salt on concentrated SSY solutions is through the structural reorganization of SSY aggregates. The aggregates are not bound by any covalent bonds (unlike the DNA molecules) and can be easily disrupted by strongly charged large counterions such as Spm^{4+}. Apparently, these modifications and disruptions of the aggregate structure suppress the ability of the system to preserve the N phase.

4.4. NaOH and Spermine in Free Base Form. Both Spm free base and NaOH increase the pH of the solutions. High pH increases the negative charge of SSY and thus weakens aggregation (a smaller $E_1 - E_e$). Gooding et al.[19] studied aggregation of SSY in dilute solutions ($c < 0.1$ mol/kg) and found that at pH ≥ 13, SSY does not aggregate at all. Taylor and Herzfeld[23] demonstrated that when E_1 decreases, the N phase disappears, giving rise to the coexisting I+C phases. At very low E_1, the system might even crystallize.[23] All these predictions are in qualitative agreement with our data, Figure 12. Namely, at low concentrations c_{NaOH} of the added base NaOH, the increased pH narrows the temperature range of the N phase. At higher c_{NaOH}, the base promotes biphasic regions I+N, I+C and a complete isotropization of the solution with precipitation of a crystalline phase at still higher c_{NaOH}, Figure 12.

Weakened aggregation at high pH is opposite to the effect of added monovalent and divalent salts that enhance molecular attractions and thus strengthen aggregates. The same consideration of pH-modified intra-aggregate attractions might apply to the case of Spm free base, but here the situation is more complicated, as with increasing pH, one also changes the state of Spm molecules themselves, most of which become neutral at high pH. These neutral Spm^0 molecules, being relatively large, act as "crowding" agents that promote inter-aggregate attraction through the "excluded volume" effect, as discussed below.

The free base form of Spm causes a similar peculiar change in the phase diagram, Figure 8b, as NaOH does, Figure 12, by first suppressing the N phase at low concentrations c_s and then replacing it with biphasic states, a densely packed N phase or even C phase, coexisting with the I phase. The latter effect cannot be explained by the multivalent-induced mechanism of electrostatic attraction, as Spm base raises the pH to the level at which its own dissociation with the formation of charged counterions is suppressed. For example, in the mixture with $c_s = 0.2$ mol/kg of Spm and $c = 1.14$ mol/kg of SSY, one finds pH = 11.3. Using the Henderson−Hasselbach equation,[69] one finds that at this pH, the majority ($\sim 70\%$) of Spm molecules exist in an undissociated, neutral form Spm^0; less than 0.01% have the charge 3+ and less than $10^{-5}\%$ have the charge 4+. At high concentration of Spm free base, the system contains mostly neutral Spm^0. The volume fraction of the latter is about 0.03, i.e., not negligible as compared to the volume fraction of SSY. At high concentrations of Spm^0, the system would phase separate into a Spm^0-rich I phase and a SSY-rich orientationally ordered phase, if the loss of the entropy of mixing is compensated by the gain in translational entropy of the components, as in the model proposed by Madden and Herzfeld.[70,71]

The model[70,71] describes demixing in a ternary system composed of a self-assembling LCLC solute, a nonaggregating solute, and a solvent (water), thus extending the Taylor−Herzfeld model.[23] The diameter of the nonaggregating spheres is close to the diameter of spherical monomers of LCLC (in our experiment, the diameter of the neutral Spm^0 is close to the diameter of the SSY "disk", 1 nm). According to the numerical simulations,[71] addition of the nonaggregating spheres to the N phase produces a wider biphasic N+I region in which a dilute I phase enriched with additives coexists with a concentrated N solution that is practically free of the additives. At high concentration of spheres, the N phase might be replaced by a wide I+C coexistence region,[71] in qualitative agreement with our data, Figure 8b.

Finally, we observed that acid HCl restores a homogeneous N phase from the I+C phase separated state created by Spm free base, Figure 10, or by NaOH. This effect falls naturally in the mechanisms addressed above. Namely, HCl-induced reduction of pH implies a decreased negative charge carried by the SSY molecules (promoting their aggregation) and an increase of the positively charge of spermine molecules. In effect, a simultaneous action of the appropriate amounts of HCl and Spm free base should be similar to the effect of SpmCl$_4$ salt, whereas simultaneous action of HCl and NaOH should resemble the effect of added NaCl, as indeed observed in the experiments.

5. Conclusions

The LCLCs exhibit unique properties for which the understanding remains rudimental. The very formation of the orientationally ordered phases in SSY represents a puzzle, because it is observed when the volume fraction of SSY and the correlation length ξ_L measured along the stacking direction are too low to satisfy the conditions of the Onsager model or its variations considering rod-like aggregates. We propose that the true structure of SSY aggregates includes morphologies more complex than simple rods, with two levels of structural hierarchy, a small scale ξ_L of correlated stacking and a larger scale of uncorrelated stacking, corresponding to the overall size of the aggregates. The larger scale is responsible for the formation of orientational order.

The behavior of LCLCs is extremely sensitive to the electrostatic effects, as we demonstrate by adding various charged species to the SSY solutions. We identify two main scenarios when a concentrated water solution of SSY is doped with additives: (a) stabilization of the N phase in the presence of mono- and divalent salts, featuring an increase of the N-to-I transition temperature and of ξ_L; the divalent salt MgSO$_4$ is capable of condensing the N phase from the initially isotropic solution of SSY; (b) suppression of the N phase with its subsequent separation into the more densely packed N phase or the C phase, both coexisting with a less condensed I phase, when bases such as NaOH and Spermine free base are added. Adding an acid to the I+C biphasic region restores a homogeneous N phase.

The observed modifications can be triggered by changes in both intra-aggregate and inter-aggregate interactions. For example, mono- and divalent salts partially screen the electrostatic repulsions within and between the aggregates, promoting aggregation that stabilizes the N phase. A higher pH increases the negative charge of the SSY molecules and thus suppresses aggregation and formation of the N phase, as demonstrated by adding NaOH to SSY solution. Excluded volume effects also should play a prominent role. Doping of the SSY solutions with Spm free base increases pH so that Spm remain neutral, yet the solution experiences a dramatic transformation, forming a biphasic I+C region from the originally homogeneous N phase. We tentatively relate this transformation to the entropy-driven demixing effect: in concentrated ("crowded") solutions, the freedom gained by segregation of particles with different packing parameters (such as SSY aggregates and neutral Spm

molecules) can exceed the mixing entropy that is lost in demixing.[72] Experiments on mapping the distribution of specially labeled additives in the different portions of biphasic regions of LCLC solutions are currently in progress to verify this hypothesis.

To conclude, there is no unifying model that could describe the observed features of phase behavior of SSY, a relatively simple representative of the LCLC class. The presented experimental data on phase diagrams in the presence of ionic additives, or even without these, demonstrate an extraordinarily rich variety of possible effects and mechanisms and can serve as a basis for further studies and eventual development of a satisfactory model.

References and Notes

(1) Vasilevskaya, A. S.; Generalova, E. V.; Sonin, A. S. Chromonic mesophases. *Uspekhi Khimii* **1989**, *57*, 1575−1596; *Russ. Chem. Rev.* **1989**, *58*, 904−916 (Engl. transl.).

(2) Lydon, J. E. Chromonic liquid crystal phases. *Curr. Opin. Colloid Interface Sci.* **1998**, *3*, 458−466; Chromonic mesophases. *Curr. Opin. Colloid Interface Sci.* **2004**, 8480−8489.

(3) Edwards, D. J.; Ormerod, A. P.; Tiddy, G. J. T.; Jaber, A. A.; Mahendrasingham, A. Aggregation and lyotropic liquid crystal formation of anionic azo dyes for textile fibres. In *Physico-Chemical Principles of Colour Chemistry*; Peters, A. T., Freeman, H. S., Eds.; Advances in color chemistry series; Springer-Verlag: New York, 1996; Vol. 4, pp 83−106.

(4) Yu, L. J.; Saupe, A. Deuteron resonance of nematic disodium cromoglycate-water systems. *Mol. Cryst. Liq. Cryst.* **1982**, *80*, 129–143.

(5) Nastishin, Y. A.; Liu, H.; Shiyanovskii, S. V.; Lavrentovich, O. D.; Kostko, A. F.; Anisimov, M. A. Pretransitional fluctuations in the isotropic phase of a lyotropic chromonic liquid crystal. *Phys. Rev. E* **2004**, *70*, 051706.

(6) Kaznatcheev, K. V.; Dudin, P.; Lavrentovich, O. D.; Hitchcock, A. P. X-ray microscopy study of chromonic liquid crystal dry film texture. *Phys. Rev. E* **2007**, *76*, 061703.

(7) Tam-Chang, S.-W.; Helbley, J.; Iverson, I. K. A study of the structural effects on the liquid-crystalline properties of ionic perylenebis-(dicarboximide)s using UV-vis spectroscopy, polarized light microscopy, and NMR spectroscopy. *Langmuir* **2008**, *24*, 2133–2139.

(8) Hartshorne, N. H.; Woodard, G. D. Mesomorphism in the system disodium chromoglycate (DSCG)-water. *Mol. Cryst. Liq. Cryst.* **1981**, *24*, 153–154.

(9) Lydon, J. E. New models for the mesophases of disodium cromoglycate (intal). *Mol. Cryst. Liq. Cryst. Lett.* **1980**, *64*, 19–24.

(10) Kostko, A. F.; Cipriano, B. H.; Pinchuk, O. A.; Ziserman, L.; Anisimov, M. A.; Danino, D.; Raghavan, S. R. Salt effects on the phase behavior, structure, and rheology of chromonic liquid crystals. *J. Phys. Chem. B* **2005**, *109*, 19126–19133.

(11) Mohanty, S.; Chou, S.-H.; Brostrom, M.; Aguilera, J. Predictive modeling of self assembly of chromonic materials. *Mol. Simul.* **2006**, *32*, 1179–1185.

(12) Prasad, S. K.; Nair, G. G.; Hegde, G.; Jayalakshmi, V. Evidence of wormlike micellar behavior in chromonic liquid crystals: Rheological, X-ray, and dielectric studies. *J. Phys. Chem. B* **2007**, *111*, 9741–9746.

(13) Ormerod, A. P. The formation of chromonic liquid crystals by water soluble azo dyes. *Ph.D. thesis*, University of Salford, Salford, U.K., 1995.

(14) Luoma, R. J. X-ray scattering and magnetic birefringence studies of aqueous solutions of chromonic molecular aggregates. *Ph.D. thesis*, Brandeis University, Waltham, MA, 1995.

(15) Horowitz, V.R.; Janowitz, L. A.; Modic, A. L.; Heiney, P. A.; Collings, P. J. Aggregation behavior and chromonic liquid crystal properties of an anionic monoazo dye. *Phys. Rev. E* **2005**, *72*, 041710.

(16) Edwards, D. J.; Jones, J. W.; Lozman, O.; Ormerod, A. P.; Sintyureva, M.; Tiddy, G. J. T. Chromonic Liquid Crystal formation by Edicol Sunset Yellow. Submitted for publication, 2008.

(17) Gooding, J. J.; Compton, R. G.; Brennan, C. M.; Atherton, J. H. The mechanism of the electro-reduction of some azo dyes. *Electroanalysis* **1996**, *8*, 519–523.

(18) Wojciechowski, K.; Szymczak, A. The research of the azo-hydrozone equilibrium by means of AM1 method based on the example of an azo dye - the Schäffer salt derivative. *Dyes Pigments* **2007**, *75*, 45–51.

(19) Gooding, J. J.; Compton, R. G.; Brennan, C. M.; Atherton, J. H. A new electrochemical method for the investigation of the aggregation of dyes in solution. *Electroanalysis* **1997**, *9*, 759–764.

(20) Wojciechowski, K.; Szymczak, A. Effect of the sulphonic group position on the properties of monoazo dyes. *Dyes Pigments* **2000**, *44*, 137–147.

(21) Gelbart, W. M.; Ben-Shaul, A. The "New" Science of "Complex Fluids". *J. Phys. Chem.* **1996**, *100*, 13169–13189.

(22) Cates, M. E.; Candau, S. J. Static and dynamics in worm-like surfactant micelles. *J. Phys.: Condens. Matter* **1990**, *2*, 6869–6892.

(23) Taylor, M. P.; Herzfeld, J. Shape anisotropy and ordered phases in reversibly assembling lyotropic systems. *Phys. Rev. A* **1991**, *43*, 1892–1905.

(24) Taylor, M. P.; Herzfeld, J. Liquid-crystal phases of self-assembled molecular aggregates. *J. Phys.: Condens. Matter* **1993**, *5*, 2651–2678.

(25) Yamada, M.; Nakamura, M.; Yamada, T.; Maitani, T.; Yukihiro, G. Structural determination of unknown subsidiary colors in food yellow No. 5 (Sunset Yellow FCF). *Chem. Pharm. Bull.* **1996**, *44*, 1624–1627.

(26) Yamada, M.; Kawahara, A.; Nakamura, M.; Nakazawa, H. Analysis of raw materials, intermediates and subsidiary colors in food yellow No. 5 (Sunset Yellow FCF) by LC/MS. *Food Additives Contaminants* **2000**, *17*, 665–674.

(27) Geall, A. J.; Taylor, R. J.; Earll, M. E.; Eaton, M. A. W.; Blagbrough, I. S. Synthesis of cholesterol polyamine carbamates: pKa studies and condensation of calf thymus DNS. *Chem. Commun.* **1998**, 1403–1404.

(28) Mao, H.; Yang, T.; Cremer, P. S. A microfluidic device with a linear temperature gradient for parallel and combinatorial measurements. *J. Am. Chem. Soc.* **2002**, *124*, 4432–4435.

(29) Hammersley, A. P.; Svensson, S. O.; Hanfland, M.; Fitch, A. N.; Häusermann, D. Two-dimensional detector software: From real detector to idealised image or two-theta scan. *High Pressure Research* **1996**, *14*, 235–248.

(30) Kleman, M.; Lavrentovich, O. D. *Soft Matter Physics: An Introduction*; Springer: New York, 2003; p 638.

(31) Collings, P. J. Swarthmore College, Swarthmore, PA. Personal communication, 2007.

(32) Herz, A. H. Aggregation of sensitizing dyes in solution and their adsorption onto silver halides. *Adv. Colloid Interface Sci.* **1977**, *8*, 237–298.

(33) Oswald, P.; Pieranski, P. *Smectic and columnar liquid crystals: concepts and physical properties illustrated by experiments*; The liquid crystal book series; CRC Press: Boca Raton, FL, 2006.

(34) Onsager, L. The effects of shape on the interaction of colloidal particles. *Ann. N. Y. Acad. Sci.* **1949**, *51*, 627–659.

(35) Rau, D. C.; Lee, B.; Parsegian, V. A. Measurement of the repulsive force between polyelectrolyte molecules in ionic solution: Hydration forces between parallel DNA double helices. *Proc. Natl. Acad. Sci. U.S.A.* **1984**, *81*, 2621–2625.

(36) Mariani, P.; Ciuchi, F.; Saturni, L. Helix-specific interactions induce condensation of guanosine four-stranded helices in concentrated salt solutions. *Biophys. J.* **1998**, *74*, 430–435.

(37) MacKintosh, F. C.; Safran, S. A.; Pincus, P. A. Self-assembly of linear aggregates: the effect of electrostatics on growth. *Europhys. Lett.* **1990**, *12*, 697–702, Note that the right-hand-parts of eqs 1 and 2 in this article are written with a factor "2", which apparently refers to a weight average as opposed to a number average value of $\langle n \rangle$.

(38) Oosawa, F. *Polyelectrolytes*; Marcel Dekker: New York, 1971.

(39) Manning, G. S. The molecular theory of polyelectrolyte solutions with applications to the electrostatic properties of polynucleotides. *Q. Rev. Biophys.* **1978**, *11*, 179–246.

(40) Grossberg, A. Y.; Nguyen, T. T.; Shklovskii, B. I. The physics of charge inversion in chemical and biological systems. *Rev. Mod. Phys.* **2002**, *74*, 329–344.

(41) Dobrynin, A. V.; Rubinstein, M. Theory of polyelectrolytes in solutions and at surfaces. *Prog. Polym. Sci.* **2005**, *30*, 1049–1118.

(42) Naji, A.; Jungblut, S.; Moreira, A. G.; Netz, R. R. Electrostatic interactions in strongly coupled soft matter. *Physica A* **2005**, *352*, 131–170.

(43) Nakata, M.; Zanchetta, G.; Chapman, B. D.; Jones, C. D.; Cross, J. O.; Pindak, R.; Bellini, T.; Clark, N. A. End-to-end staking and liquid crystal condensation of 6- to 20-base pair DNA duplexes. *Science* **2007**, *318*, 1276–1279.

(44) Bolhius, P.; Frenkel, D. Tracing the phase boundaries of hard spherocylinders. *J. Chem. Phys.* **1997**, *106*, 666–687.

(45) Vroege, G. J.; Lekkerkerker, H. N. W. Phase transitions in lyotropic colloidal and polymer liquid crystals. *Rep. Prog. Phys.* **1992**, *55*, 1241–1309.

(46) Stroobants, A.; Lekkerkerker, H. N. W.; Odijk, T. Effect of electrostatic interaction on the liquid crystal phase transition in solutions of rodlike polyelectrolytes. *Macromolecules* **1986**, *19*, 2232–2238.

(47) Potemkin, I. I.; Limberger, R. E.; Kudlay, A. N.; Khokhlov, A. R. Rodlike polyelectrolyte solutions: Effect of the many-body coulomb attraction of similarly charged molecules favoring weak nematic ordering at very small polymer concentration. *Phys. Rev. E* **2002**, *66*, 011802.

(48) Potemkin, I. I.; Oskolkov, N. N.; Khokhlov, A. R.; Reineker, P. Effect of low-molecular-weight salt on the nematic ordering in solutions of rodlike polyelectrolytes. *Phys. Rev. E* **2002**, *72*, 021804.

(49) Khokhlov, A. R.; Semenov, A. N. Liquid-crystalline ordering in the solution of long persistent chains. *Physica A* **1981**, *108A*, 546–556.

(50) Selinger, J. V.; Bruinsma, R. F. Hexagonal and nematic phases of chains. 2. Phase transitions. *Phys. Rev. A* **1991**, *43*, 2922–2931.

(51) Shundyak, K.; van Roji, R.; van der Schoot, P. Theory of the isotropic-nematic transition in dispersions of compressible rods. *Phys. Rev. E.* **2006**, *74*, 021710.

(52) Lu, X.; Kindt, J. T. Monte Carlo simulations of self-assembly and phase behavior of semiflexible equilibrium polymers. *J. Chem. Phys.* **2004**, *120*, 10328–10338.

(53) Jain, S.; Bates, F. C. On the origins of morphological complexity in block copolymer surfactants. *Science* **2003**, *300*, 460–464.

(54) Dan, N.; Shimoni, K.; Pata, V.; Danino, D. Effect of Mixing on the Morphology of Cylindrical Micelles. *Langmuir* **2006**, *22*, 9860–9865.

(55) Schneider, T.; Artyushkova, K.; Fulghum, J. E.; Broadwater, L.; Smith, A.; Lavrentovich, O. D. Oriented monolayers prepared from lyotropic chromonic liquid crystal. *Langmuir* **2005**, *21*, 2300–2307.

(56) Zilman, A. G.; Safran, S. A. Thermodynamics and structure of self-assembled networks. *Phys. Rev. E* **2002**, *66*, 051107.

(57) Israelachvili, J. *Intermolecular and Surface Forces*, 2nd ed.; Academic Press: London, 1992; p 450.

(58) Srinivasan, V.; Blankschtein, D. Effect of counterion binding on micellar solution behavior: 2. Prediction of micellar solution properties of ionic surfactant - electrolyte systems. *Langmuir* **2003**, *19*, 9946–9961.

(59) Qiu, X.; Andersen, K.; Kwok, L. W.; Lamb, J. S.; Park, H. Y.; Pollack, L. Inter-DNA attraction mediated by divalent counterions. *Phys. Rev. Lett.* **2007**, *99*, 038104.

(60) Bloomfield, V. A. DNA condensation. *Curr. Opin. Struct. Biol.* **1996**, *6*, 334–345, and references therein.

(61) Raspaud, E.; Durand, D.; Livolant, F. Interhelical spacing in liquid crystalline spermine and spermidine-DNA precipitates. *Biophys. J.* **2005**, *88*, 392–403.

(62) Burak, Y.; Ariel, G.; Andelman, D. Competition between condensation of monovalent and multivalent ions in DNA aggregation. *Curr. Opin. Colloid Interface Sci.* **2004**, *9*, 53–58.

(63) Dai, L.; Mu, Y.; Nordenskiold, L.; van der Maarel, J. R. C. Molecular dynamics simulation of multi-valent-ion mediated attraction between DNA molecules. *Phys. Rev. Lett.* **2008**, *100*, 118301.

(64) Faraudo, J.; Travesset, A. The many origins of charge inversion in electrolyte solutions: Effects of discrete interfacial charges. *J. Phys. Chem. C* **2007**, *111*, 987–994.

(65) Chattoraj, D. K.; Gosule, L. C.; Schellman, J. A. DNA condensation with polyamines. *J. Mol. Biol.* **1978**, *121*, 327–337.

(66) Pelta, J.; Durand, D.; Doucet, J.; Livolant, F. DNA mesophases induced by spermine: Structural properties and biological implications. *Biophys. J.* **1996**, *71*, 48–63.

(67) Vijayanathan, V.; Lyall, J.; Thomas, T.; Shirahata, A.; Thomas, T. J. Ionic, structural and temperature effects on DNA nanoparticles formed by natural and synthetic polyamines. *Biomacromolecules* **2005**, *6*, 1097–1103.

(68) Borukhov, I.; Bruinsma, R. F.; Gelbart, W. M.; Liu, A. J. Structural polymorphism of the cytoskeleton: A model of linker-assisted filament aggregation. *Proc. Natl. Acad. Sci.* **2005**, *102*, 3673–3678.

(69) Harris, D. C. *Quantitative Chemical Analysis*, 4th ed.; W. H. Freeman and Co.: New York, 1995; pp 263−265.

(70) Madden, T. L.; Herzfeld, J. Exclusion of spherical particles from the nematic phase of reversibly assembled rod-like particles. *Mater. Res. Soc. Symp. Proc.* **1992**, *248*, 95–101.

(71) Madden, T. L.; Herzfeld, J. Liquid crystal phases of self-assembled amphiphilic aggregates. *Philos. Trans. R. Soc. London A* **1993**, *344*, 357–375.

(72) Herzfeld, J. Crowding-induced organization in cells: Spontaneous alignment and sorting of filaments with physiological control points. *J. Mol. Recognit.* **2004**, *17*, 367–381.